Thermoelectric Materials

DOI: 10.1002/ange.200600848

Nanostructured Bi_2Se_3 Films and Their Thermoelectric Transport Properties**

Xiaofeng Qiu, Leah N. Austin, Philip A. Muscarella, Jeffrey S. Dyck,* and Clemens Burda*

Since the discovery of the thermoelectric effect by Thomas Johann Seebeck in 1821, solid-state thermoelectric materials have long held the promise of becoming the next generation of energy converters thanks to their small size, light weight, reliability, and potential for higher conversion efficiencies.[1] However, bulk thermoelectric materials seem to have reached their performance limit; most materials exhibit an optimum thermoelectric figure of merit (ZT) of about 1 at room temperature, which equates to only around 10% of the Carnot efficiency. Since the 1960s, the efficiencies of bulk thermoelectric materials have been improved only marginally. To promote the economic potential of these materials and to support the full development of the associated technological applications, improvements in thermoelectric efficiencies leading to $ZT \geq 3$ at room temperature are required. It was not until the early 1990s that Dresselhaus and co-workers demonstrated theoretically that it is possible to increase the ZT values drastically by decreasing the size of thermoelectric materials.[2–5] However, the practical difficulties in synthesizing, testing, and utilizing structures smaller than 100 nm make the production of nanoscale thermoelectric materials a real challenge. Therefore, methods that provide reproducible and stable nanostructured thermoelectric films and reliable thermoelectric measurements are of great importance. We have developed chemically grown nanostructured thermoelectric films, the building and testing of which is a significant step towards better thermoelectric materials.

Only a few nanostructured thermoelectric devices with significant improvement of ZT values have been reported. Venkatasubramanian et al. successfully prepared Bi_2Te_3/Sb_2Te_3 superlattice thin films by molecular-beam epitaxy and obtained a ZT value of 2.4 at room temperature.[6] Harman et al. achieved a ZT value of 2.0 at 300 K with PbSeTe-based quantum-dot superlattice structures grown by a similar method.[7] However, the techniques that were used to produce these superlattice structures are very delicate and exceedingly expensive and therefore are unlikely to be applicable to large-scale production. In the meantime, a cheaper and easier pressure-injection method using an alumina template was developed to prepare Bi and $Bi_{1-x}Sb_x$ alloy nanowire arrays and their thermoelectric properties were investigated.[8–11] A related template-based electrochemical method was used to produce a group of high-ZT thermoelectric materials.[12–15] The alumina-template-based nanowire arrays are an important step towards establishing nanostructures with possible high thermoelectric performance. However, no significant improvement in ZT value was reported and the template materials were suspected to cause complications for transport measurements.[16]

Herein, we introduce an alternative strategy to grow nanostructures on a wide variety of substrates and perform thermoelectric measurements on these nanostructured films. The synthesis is based on a previously reported Bi_2Se_3 preparation[17,18] and a method by Vayssieres for growing thin films.[19] The synthesis involves the reduction of a selenium precursor (Na_2SeSO_3) by ascorbic acid to promote nucleation with nitrilotriacetic acid (NTA) coordinated Bi^{3+}, which deposits Bi_2Se_3 nanostructures on the substrates. Since the reduction potential of ascorbic acid is pH-dependent and the equilibrium between NTA and Bi^{3+} determines the availability of free Bi^{3+} ions, the growth of Bi_2Se_3 can be thermodynamically controlled. Other important parameters such as temperature and reaction time also provide further control over the nanostructure growth. Another very important factor is the surface charge density, which alters the interfacial tension.[19] Control of this parameter was accomplished by adjusting the pH value and the ionic strength of the reaction mixture. This method allows the production of films with different composition, grain size, and thickness, as well as deposition on substrates of any size, shape, and composition. This versatility constitutes an important improvement in the preparation of thermoelectric thin films and opens up the possibility for a range of applications.

To avoid the complications of unwanted parallel electrical and thermal conductance from substrates, all Bi_2Se_3 thin films herein were grown on glass substrates, although the results did not depend on the choice of substrate. The thin films prepared by this method exhibit hexagonal structure (JCPDS file: 33-214), as shown in Figure 1. No impurity phases were detected in the X-ray data. The stable baseline and sharp diffraction peaks indicate that the thin film produced shows significant coverage of the substrate and is highly crystalline. Ensuring reproducibly high quality films was a major concern in developing the presented experiments, since only continuous and highly crystalline thin films allow successful measurements.

Figure 2 shows the scanning electron microscopy (SEM) images of the Bi_2Se_3 nanostructured thin films. The growth process of the films can be monitored by taking images at different stages of the growth (Scheme 1). Initially, a few

---

[*] L. N. Austin, P. A. Muscarella, Prof. J. S. Dyck
Department of Physics
John Carroll University
20700 North Park Blvd.
University Heights, OH 44118 (USA)
Fax: (+1) 216-397-4499
E-mail: jdyck@jcu.edu

X. Qiu, Prof. C. Burda
Center for Chemical Dynamics and Nanomaterials Research
Department of Chemistry
Case Western Reserve University
10900 Euclid Avenue, Cleveland, OH 44106 (USA)
Fax: (+1) 216-368-3006
E-mail: burda@case.edu

[**] C.B. acknowledges support from the NSF (#CHE-0239688), an ACS-PRF (#45359-AC10), and the Ohio Board of Regents.

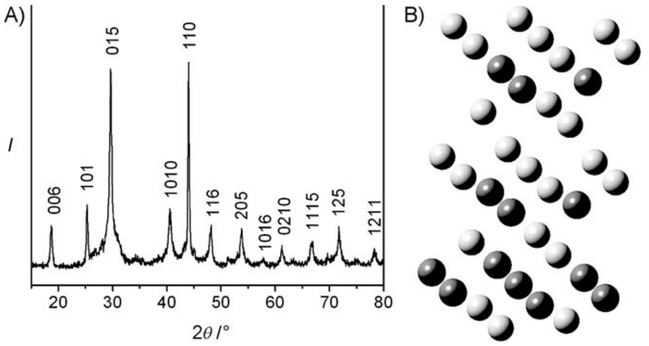

Figure 1. A) XRD pattern of the prepared nanostructured Bi_2Se_3 thin film. B) 3D crystal structure of Bi_2Se_3; black: Bi, gray: Se.

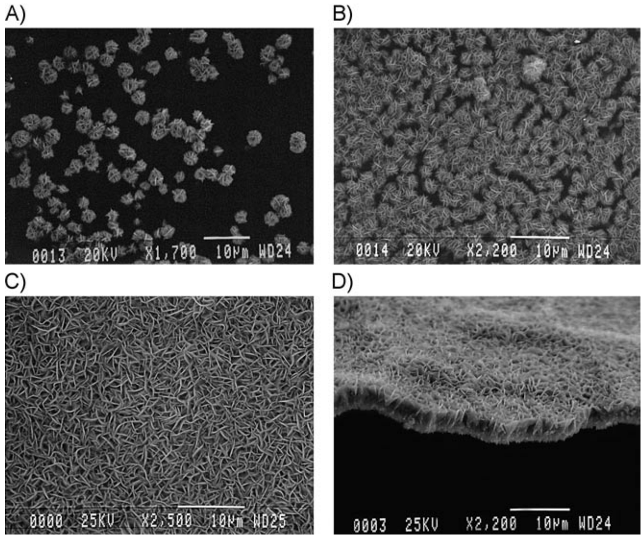

Figure 2. SEM images of the synthesized films showing the increasing coverage of the substrate. A) After 5 min. B) After 30 min. C) After 120 min. D) Cross-sectional view of the thin film.

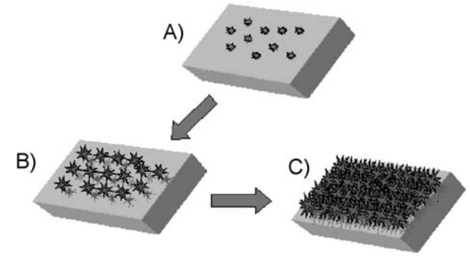

Scheme 1. Steps observed during film growth. A) Initial nucleation; B) Coalescence; C) Lamella-structured film formation.

Bi_2Se_3 nucleation centers form and quickly develop into starlike structures (Scheme 1, step A and Figure 2a). As the number of nucleation centers increases, the rapidly developing starlike structures start to grow into each other (Scheme 1, step B and Figure 2b). After a growth time of typically 3 h, the individual island structures coalesce and form a continuous lamella-structured film (Scheme 1, step C and Figure 2c). The thickness of the individual lamella structures does not change during the growth period and remains in the range 30–80 nm. This observation indicates that the surface charge density may be at a maximum; thus the interfacial tension results in a minimum.[19] Under such conditions the lamella thickness remains less than 100 nm. Furthermore, the thickness of the film is very uniform but can be varied by changing the concentrations of the precursors. This indicates that the growth along the film surface is uniform, which in turn supports a more uniform charge-carrier transport through the nanostructured film.

To perform reproducible thermoelectric measurements and obtain reliable data from the nanostructured thin films requires synthetic reproducibility. A major concern in the measurements is to avoid additional conductance from substrates as well as other side effects; therefore, the prepared thin films should be grown on a substrate with very low electrical and thermal conductance. This requirement constitutes a problem for most electrochemical deposition techniques. We used glass slides as substrates to avoid parallel currents through substrates or other chemical residues of the synthesis that were encountered in earlier experiments.[16]

Figure 3 displays the resistance (R) and Seebeck coefficient (S) of a Bi_2Se_3 film from 6 to 300 K. These data are representative of values obtained for these films. The Seebeck coefficient is negative and has linear temperature dependence. Negative values of S indicate n-type conduction, which is expected for Bi_2Se_3, which typically has a high density of selenium vacancies.[20] The value at room temperature ($-119\ \mu V K^{-1}$) is larger by a factor of two than that found for bulk, single crystals with electron concentration $n \approx 10^{20}\ cm^{-3}$ grown by the Bridgman method,[21] and very similar to that reported for polycrystalline Bi_2Se_3 with $n \approx 10^{19}\ cm^{-3}$ grown by metal–organic chemical vapor deposition (MOCVD).[22] The thermoelectric figure of merit is determined by a dimensionless parameter $ZT = S^2 T/\rho\kappa$, in which ρ is the electrical resistivity and κ is the thermal conductivity. Enhanced S values can directly contribute to an increase of the ZT value.

Electrical-resistance measurements of the thin films were also performed over a wide temperature range, and it was

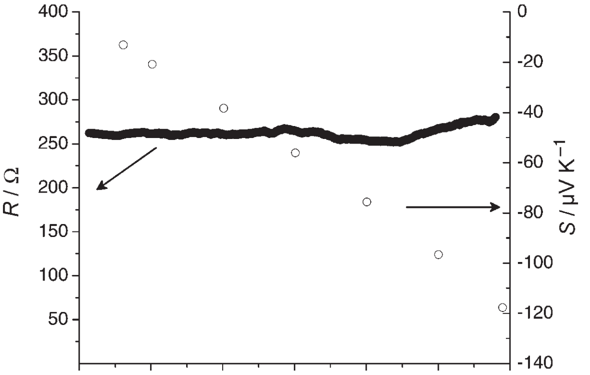

Figure 3. Solid circles, left axis: Electrical resistance (R) of a nanostructured Bi_2Se_3 thin film from 6 to 300 K. Open circles, right axis: Seebeck coefficients (S) between 30 and 300 K for the same Bi_2Se_3 thin film. The negative temperature dependence of S indicates dominant n-type conduction.

found that R has a minimal dependence on temperature. The resistance increases about 30 Ω as the temperature rises from 6 to 300 K. To calculate ρ, one needs to know the exact current density. For mesoporous thin films, it is extremely difficult to measure the exact cross-sectional area precisely. However, quite certainly, ρ of the thin film is higher than that of a single crystal. A higher electrical resistivity will counteract the ZT enhancement that results from a larger Seebeck coefficient. Unfortunately, this situation is common for nanoscale thermoelectric materials since an increase in S generally means an increase in ρ.

The nanostructured films should efficiently reduce the thermal conductivity κ of the thin film. It is evident from the relationship $ZT = S^2 T/\rho\kappa$ that a decrease in κ enhances the thermoelectric figure of merit. The thermal conductivity κ_{tot} is the sum of components deriving from electronic (κ_{el}) and lattice (κ_{lat}) contributions. The electronic thermal contribution can be ignored for our measurements, since the electrical resistivity is high. Therefore, only the lattice thermal conductivity is relevant in this case and $\kappa_{tot} \approx \kappa_{lat}$. Furthermore, the lamella-type structures will drastically increase the density of boundaries in the film, thus causing boundary phonon scattering and a further decrease in κ_{lat}.[23] Therefore, the experimental κ_{lat} value for our nanostructured thin films should certainly be lower than the known value for single bulk crystals ($\kappa_{lat} = 1.33\ \mathrm{W\,m^{-1}\,K^{-1}}$ in the direction perpendicular to the c axis at room temperature), which makes the total thermal conductivity κ_{tot} of the presented film much lower than the bulk value. Future experiments will be aimed at determining the thermal conductivity; it is expected that the significant decrease of the κ value allows the ultimate ZT value to be improved. Furthermore, the ease with which the thin film structures can be chemically controlled provides additional possibilities to increase ZT values.

In summary, we have introduced a new chemical method to produce nanostructured films for thermoelectric studies and applications. Varying the synthetic parameters allows control of the scale, morphology, and composition of the films and enables the thermoelectric transport properties to be optimized reliably and less expensively. This method should also allow large-scale production of functional thin films for applications such as catalysis and energy conversion.

Experimental Section

The glass substrate ($22 \times 40\ \mathrm{mm^2}$; Corning Glass Works (USA)) was cut into strips ($2 \times 8\ \mathrm{mm^2}$) with a diamond cutter, cleaned with ethanol, acetone, and distilled water, and then dried in air. A typical precursor solution is composed of nitrilotriacetic acid (NTA; 4.0 g; Aldrich, 99+%), ascorbic acid (1.0 g; Aldrich, 99%), $Bi(NO_3)_3{\cdot}5H_2O$ (0.5 g; Sigma-Aldrich, 99.99%), and freshly made Na_2SeSO_3 solution (8 mL). The glass slides were placed into a teflon-capped flask and heated at 60°C for 2 h. A uniform film was formed on the surface of the glass slides. The thin films were rinsed several times with distilled water to remove any excess precipitates and then dried.

The phase purity of the thin films was analyzed with a Scintag X-1 Advanced X-ray diffractometer (XRD, 2.4° min^{-1}, $Cu_{K\alpha}$ radiation), and the morphology of the thin films was characterized with a JOEL JFM-840 scanning electron microscope (20 kV, JEOL, Japan).

The electrical resistance (R) and Seebeck coefficient (S) were measured in the plane of the film as a function of temperature upon warming. The sample thickness was typically in the range 1–5 μm. The sample temperature was controlled with a closed-cycle helium refrigerator equipped with a radiation shield, and the sample space was kept at pressures below 10^{-5} Torr. Electrical resistance was measured in a four probe configuration by using a SRS 830 lock-in amplifier (Stanford Research Systems, Inc. USA) with an excitation frequency of 16 Hz. The excitation currents, determined with a Keithley 195 A multimeter (Keithley Instruments Inc. USA), were kept below 50 μA to prevent sample damage and heating. The average warming rate for the resistance measurements was less than 1 K min^{-1}. For the measurements of the Seebeck coefficients, one end of the sample was thermally anchored with GE 7031 varnish (Cambridge Magnetic Refrigeration, UK) to a copper cold sink, and a miniature strain gauge mounted at the free end of the sample served as heater. Thermal gradients with magnitude of less than 5% of the absolute temperature were measured with the aid of fine copper-constantan thermocouples, and the copper legs of the thermocouples were used to measure the sample voltage. Keithley 2182 nanovoltmeters (Keithley Instruments Inc. USA) were used to measure the sample voltage and thermocouple voltages. Seebeck coefficients were determined from the slope of plots of sample voltage versus ΔT while holding the cold end of the sample at a constant temperature. Electrical contacts to the sample were made by using colloidal silver paste (Ted Pella, USA) to avoid heating the sample with solder.

Received: March 6, 2006

Keywords: nanostructures · thermoelectric materials · thin films · transport properties

---

[1] F. J. DiSalvo, *Science* **1999**, *285*, 703–706.
[2] L. D. Hicks, M. S. Dresselhaus, *Phys. Rev. B* **1993**, *47*, 12727–12731.
[3] L. D. Hicks, M. S. Dresselhaus, *Phys. Rev. B* **1993**, *47*, 16631–16634.
[4] M. S. Dresselhaus, Y. M. Lin, S. B. Cronin, O. Rabin, M. R. Black, D. Dresselhaus, T. Koga, *Semicond. Semimetals* **2001**, *71*, 1–121.
[5] Y. M. Lin, M. S. Dresselhaus, *Phys. Rev. B* **2003**, *68*, 075304.
[6] R. Venkatasubramanian, E. Silvola, T. Colpitts, B. O'Quinn, *Nature* **2001**, *413*, 597–602.
[7] T. C. Harman, P. J. Taylor, M. P. Walsh, B. E. LaForge, *Science* **2002**, *297*, 2229–2232.
[8] Z. Zhang, J. Y. Ying, M. S. Dresselhaus, *J. Mater. Res.* **1998**, *13*, 1745–1748.
[9] Y. M. Lin, S. B. Cronin, J. Y. Ying, M. S. Dresselhaus, J. P. Heremans, *Appl. Phys. Lett.* **2000**, *76*, 3944–3946.
[10] O. Rabin, Y. M. Lin, M. S. Dresselhaus, *Appl. Phys. Lett.* **2001**, *79*, 81–83.
[11] Y. M. Lin, O. Rabin, S. B. Cronin, J. Y. Ying, M. S. Dresselhaus, *Appl. Phys. Lett.* **2002**, *81*, 2403–2405.
[12] A. L. Prieto, M. S. Sander, M. S. Martín-González, R. Gronsky, T. Sands, A. M. Stacy, *J. Am. Chem. Soc.* **2001**, *123*, 7160–7161.
[13] M. Martín-González, A. L. Prieto, R. Gronsky, T. Sands, A. M. Stacy, *Adv. Mater.* **2003**, *15*, 1003–1006.
[14] A. L. Prieto, M. Martín-González, J. Keyani, R. Gronsky, T. Sands, A. M. Stacy, *J. Am. Chem. Soc.* **2003**, *125*, 2388–2389.
[15] M. Martín-González, G. J. Snyder, A. L. Prieto, R. Gronsky, T. Sands, A. M. Stacy, *Nano Lett.* **2003**, *3*, 973–977.
[16] R. F. Service, *Science* **2004**, *306*, 806–807.
[17] X. F. Qiu, J. J. Zhu, L. Pu, Y. Shi, Y. D. Zheng, H. Y. Chen, *Inorg. Chem. Commun.* **2004**, *7*, 319–321.

[18] X. F. Qiu, C. Burda, R. L. Fu, L. Pu, H. Y. Chen, J. J. Zhu *J. Am. Chem. Soc.* **2004**, *126*, 16276 – 16277.
[19] L. Vayssieres, *Int. J. Nanotechnol.* **2004**, *1*, 1 – 41.
[20] J. Horak, J. Navratil, Z. Stary, *J. Phys. Chem. Solids* **1987**, *48*, 1227 – 1233.
[21] J. Navratil, J. Horak, T. Plechacek, S. Kamba, P. Lostak, J. S. Dyck, W. Chen, C. Uher, *J. Solid State Chem.* **2004**, *177*, 1704 – 1712.
[22] A. Al Bayaz, A. Giani, A. Foucaran, F. Pascal-Delannoy, A. Boyer, *Thin Solid Films* **2003**, *441*, 1 – 5.
[23] M. S. Toprak, C. Stiewe, D. Platzek, S. Williams, L. Bertini, E. Muller, C. Gatti, Y. Zhang, M. Rowe, M. Muhammed, *Adv. Funct. Mater.* **2004**, *14*, 1189 – 1196.